Mineralogy and Petrology (2019) 113:7–16
https://doi.org/10.1007/s00710-018-0623-6

ORIGINAL PAPER

Description and recognition of potassic-richterite, an amphibole supergroup mineral from the Pajsberg ore field, Värmland, Sweden

Dan Holtstam[1] · Fernando Cámara[2] · Henrik Skogby[1] · Andreas Karlsson[1] · Jörgen Langhof[1]

Received: 17 April 2018 / Accepted: 12 July 2018 / Published online: 10 August 2018

Abstract

Potassic-richterite, ideally $^{A}K^{B}(NaCa)^{C}Mg_5{}^{T}Si_8O_{22}{}^{W}(OH)_2$, is recognized as a valid member of the amphibole supergroup (IMA-CNMNC 2017–102). Type material is from the Pajsberg Mn-Fe ore field, Filipstad, Värmland, Sweden, where the mineral occurs in a Mn-rich skarn, closely associated with mainly phlogopite, jacobsite and tephroite. The megascopic colour is straw yellow to grayish brown and the luster vitreous. The nearly anhedral crystals, up to 4 mm in length, are pale yellow (non-pleochroic) in thin section and optically biaxial (−), with $\alpha = 1.615(5)$, $\beta = 1.625(5)$, $\gamma = 1.635(5)$. The calculated density is 3.07 g·cm^{-1}. VHN_{100} is in the range 610–946. Cleavage is perfect along {110}. EPMA analysis in combination with Mössbauer and infrared spectroscopy yields the empirical formula $(K_{0.61}Na_{0.30}Pb_{0.02})_{\Sigma 0.93}(Na_{1.14}Ca_{0.79}Mn_{0.07})_{\Sigma 2}(Mg_{4.31}Mn_{0.47}Fe^{3+}{}_{0.20})_{\Sigma 5}(Si_{7.95}Al_{0.04}Fe^{3+}{}_{0.01})_{\Sigma 8}O_{22}(OH_{1.82}F_{0.18})_{\Sigma 2}$ for a fragment used for collection of single-crystal X-ray diffraction data. The infra-red spectra show absorption bands at 3672 cm^{-1} and 3736 cm^{-1} for the α direction. The crystal structure was refined in space group $C2/m$ to $R1 = 3.6\%$ [$I > 2\sigma(I)$], with resulting cell parameters $a = 9.9977(3)$ Å, $b = 18.0409(4)$ Å, $c = 5.2794(2)$ Å, $\gamma = 104.465(4)°$, $V = 922.05(5)$ Å^3 and $Z = 2$. The A and $M(4)$ sites split into $A(m)$ (K^+), $A(2/m)$ (Na^+), $A(2)$ (Pb^{2+}), and $M(4')$ (Mn^{2+}) subsites, respectively. The remaining Mn^{2+} is strongly ordered at the octahedrally coordinated $M(2)$ site, possibly together with most of Fe^{3+}. The skarn bearing potassic-richterite formed at peak metamorphism, under conditions of low SiO_2 and Al_2O_3 activities and relatively high oxygen fugacities.

Keywords Potassic-richterite · Amphibole supergroup · Crystal structure · Skarn · Pajsberg · Långban-type deposit · Sweden

Introduction

Potassic-richterite [ideally $K(NaCa)Mg_5Si_8O_{22}(OH)_2$, derived from the root species richterite via the homovalent substitution $^{[A]}Na^+ \rightarrow {}^{[A]}K^+$], is not a new mineral in the sense that amphibole of this composition never has been reported before; on the contrary, already in the 19th and early 20th centuries, published wet-chemical analyses indicated the existence of K-dominant amphibole varieties in what is now defined as the richterite compositional space. The analysed specimens from this period were mainly from the Långban Mn-Fe deposit, Sweden (Magnusson 1930; Sundius 1945), the type locality for richterite. There are also plenty of results from the microprobe era proving amphibole compositions approaching potassic end-member composition. Identified samples of potassic-richterite (commonly referred to as "potassium richterite" or "K-richterite" in the literature) are typically from ultrapotassic mantle-derived rocks such as peridotite xenoliths (in kimberlite) and lamproites (e.g, Erlank and Finger 1970; Dawson and Smith 1982; Wagner and Velde 1986; Mitchell 2012). The species was also reported from the metamorphosed Praborna manganese ore deposit, Val d'Aosta, Italy (Mottana and Griffin 1986; specimen later studied by single-crystal X-ray diffraction by Oberti et al. 1992). A Sr-bearing potassic-richterite from the Murun alkaline Massif (Eastern-Siberian Region, Russia) was structurally characterized by Sokolova et al. (2000).

The F-analogue, potassic-fluoro-richterite, was described by Della Ventura et al. (1992) from a volcanic ejectum from

Editorial handling: N. V. Chukanov

Electronic supplementary material The online version of this article (https://doi.org/10.1007/s00710-018-0623-6) contains supplementary material, which is available to authorized users.

✉ Dan Holtstam
dan.holtstam@nrm.se

[1] Department of Geosciences, Swedish Museum of Natural History, Box 50007, SE-104 05 Stockholm, Sweden

[2] Dipartimento di Scienze della Terra 'A. Desio', Università degli Studi di Milano, Via Luigi Mangiagalli 34, 20133 Milan, Italy

a pyroclastic deposit, Monte Somma, Italy. A K-rich richteritic amphibole with $Fe^{2+} > Mg$ ("potassic-ferro-richterite") is indicated by some analyses (e.g, Hogarth 1997), but is not yet approved. Potassic-richterite is not to be confused with "KK-richterite", a synthetic ultrahigh-pressure amphibole of composition $K(KCa)Mg_5Si_8O_{22}(OH)_2$ (e.g, Yang et al. 1999). Mazdab (2003) reviewed the diversity of K-dominant amphiboles and pointed out the need for complete characterization to achieve species status for some members.

The present paper presents data for the designated holotype specimen of potassic-richterite, approved as a valid species by the International Mineralogical Association-Commission on New Minerals, Nomenclature and Classification (IMA-CNMNC 2017–102); the name complies with the current IMA nomenclature for the amphibole supergroup (Hawthorne et al. 2012). Holotype material is deposited in the mineral collections of the Department of Geosciences, Swedish Museum of Natural History (GEO-NRM), Box 50007, SE-10405 Stockholm, Sweden, under collection number 19311387.

Description and characterisation of potassic-richterite

Occurrence and paragenesis

On the original label of the type specimen, it is written "Pajsberg iron and manganese ore mines", which could either mean the Stora Pajsberg mine (59 °47.04' N; 14 °19.03′ E), or the Harstigen mine (59 °47.10' N, 14 °18.84 'E) 200 m to the NW. Both mines belong to the Pajsberg ore field near the northernmost tip of Lake Yngen (200 m a.s.l.), Filipstad, Värmland, Sweden. However, the present sample shows the greatest physical resemblance to skarn from the Stora Pajsberg mine. It was originally collected by the mineralogist Lars Johan Igelström, probably in the 1850s, and later acquired by the chemist Johan Fredrik Lundberg. It was finally incorporated in the mineral collection of the Swedish Museum of Natural History in 1931, as "manganophyllite (manganoan phlogopite) with richterite". The occurrence of "richterite" from Pajsberg was first reported by Igelström (1867), as a common component of Mn-skarn associated with tephroite and phlogopite. Igelström's original chemical analyses of amphibole were of a semi-quantitative character, with only the sum of alkalis ($Na_2O + K_2O$) given.

The mines are located in Långban-type Mn-Fe oxide deposits hosted by dolomitic marble, with spatially separated Mn (hausmannite) and Fe (hematite-magnetite) ores, surrounded by dominantly felsic metavolcanic and metavolcaniclastic rocks. According to Hamberg (1890), richterite belongs to a group of earliest formed skarn minerals (olivine, garnet, pyroxene, rhodonite, amphibole) at the Harstigen deposit, followed by various Mn, Pb, Ba, As, Sb, and Be minerals (hydrous silicates, carbonates, sulphates, arsenates, oxyhalides, sulphides, native elements) formed in fissures and cavities at lower temperatures. Generally, the Paleoproterozoic Långban-type deposits in the Bergslagen ore region originally deposited as chemical precipitates from volcanogenic hydrothermal solutions in a shallow submarine environment (Boström et al. 1979; Holtstam and Mansfeld 2001). Subsequent episodes of hydrothermal alteration, metamorphism and deformation spanning 1.9–1.0 Ga led to the present-day skarn and late-stage mineral assemblages.

In the sample under study (Fig. 1), potassic-richterite occurs with manganoan tetraferrian phlogopite, magnesian tephroite, jacobsite and minor oxyplumboroméite in a compact, Mn-rich skarn, as masses of randomly arranged crystals. About ¼ by volume of the specimen, ca 8 × 7 × 5 cm in size, constitutes the amphibole, which shows a relatively sharp transition to a more fine-grained matrix of mainly phlogopite, jacobsite and minor calcite. Tephroite (ca 85 mol% Mn_2SiO_4 according to energy dispersive X-ray microanalysis) forms irregular, sometimes elongated grains up to 0.5 mm that have partly developed along [001] of the amphibole, and jacobsite ($Mn^{2+}[Fe^{3+}_{1.76}Mn^{3+}_{0.24}]O_4$ from microprobe data) occurs as mostly equigranular inclusions of up to 100 μm in diameter (Fig. 2).

Appearance and physical properties

Potassic-richterite exhibits a short-prismatic morphology; the crystals are subhedral to anhedral and commonly elongated along [001] with average crystal size of 1–2 mm, exceptionally up to 4 mm long. The crystals are vitreous translucent, with a straw yellow to brown colour, and a greyish white streak. In thin (ca 50 μm) crystal sections, potassic-richterite is transparent and pale yellow with no visible pleochroism. No fluorescence effects have been observed under ultraviolet light. Optically the mineral is biaxial negative, with

Fig. 1 Image of potassic-richterite with jacobsite (black, granular). Sample GEO-NRM #19311137

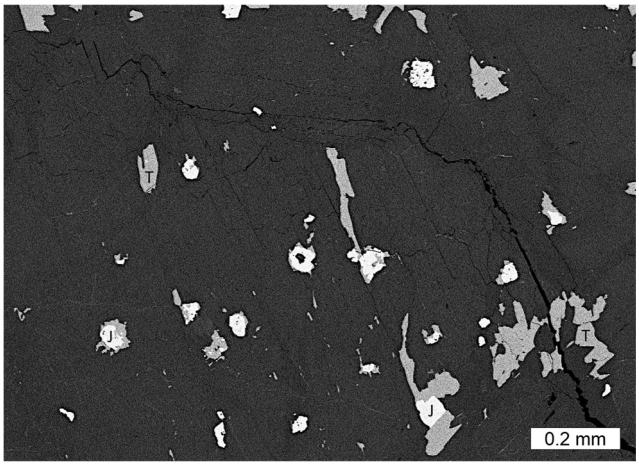

Fig. 2 Field-emission BSE image of potassic-richterite and associated minerals (J = jacobsite, T = tephroite)

$\alpha = 1.615(5)$ $\beta = 1.625(5)$ $\gamma = 1.635(5)$ (white light) and $2V_{meas} = 75(5)°$ and $Z \wedge c \sim 24$ °. Dispersion is weak, $r < v$.

Potassic-richterite is brittle, with measured Vickers hardness number (VHN_{100}) between 610 and 946 (average 806; $n = 10$) corresponding to a Mohs hardness of 5–6, and has an uneven, splintery fracture. Cleavage is perfect along {110}. The density could not be measured directly due to the foreign mineral inclusions in the crystals. The calculated value is 3.075 g·cm^{-3} (ideal formula and unit-cell parameters from X-ray single-crystal data), or 3.070 g·cm^{-3} (empirical formula and unit-cell parameters from powder X-ray diffraction data). The Gladstone-Dale compatibility (Mandarino 1981) is 1-(K_P/K_C) = 0.016 (superior category).

Chemical composition

The chemical composition of potassic-richterite was first determined from point analyses on a polished surface using an ARL-SEMQ electron probe micro-analyser (EPMA) in wavelength dispersive (WDS) mode (15 kV, 12 nA, beam size 1–2 μm), with calibrant materials: (Na, Ca Mg, Al, Si) hornblende-type melt glass, K orthoclase, Fe hematite, Mn rhodonite, F topaz. A second analysis was done with a JEOL 8200 Super Probe (WDS mode, 15 kV, 5 nA, 1 μm beam) with calibrant materials: F hornblende, Sr celestine, Mn rhodonite, K orthoclase, Pb galena, Fe fayalite, (Ca, Si, Al) grossular, Cr metal, Ni nickeline, Ti ilmenite, Mg olivine, Ba sanbornite on the fragment used for the single-crystal study. Results are given in Table 1.

The presence of $(OH)^-$ is confirmed by Fourier-transform infrared (FTIR) spectroscopy and crystal-structure refinement, see below. Complementary analysis of other light elements (Li, B, F) was done by nuclear-reaction analysis at the proton-beamline facility (LIBAF) at Lund University, Sweden (Nilsson et al. 2017; De La Rosa et al. 2017). The results (in ppm) are: Li 18 ± 4, B 104 ± 6 and F 6440 ± 480.

The average empirical formula based on 24 (O + OH + F) for the crystal fragment used in structure refinement is $(\mathbf{K}_{0.61}Na_{0.30}Pb_{0.02})_{\Sigma 0.93}(\mathbf{Na}_{1.14}\mathbf{Ca}_{0.79}Mn_{0.07})_{\Sigma 2}(\mathbf{Mg}_{4.31}Mn_{0.47}Fe^{3+}_{0.20})_{\Sigma 5}(\mathbf{Si}_{7.95}Al_{0.04}Fe^{3+}_{0.01})_{\Sigma 8}\mathbf{O}_{22}(\mathbf{OH}_{1.82}F_{0.18})_{\Sigma 2}$, where essential components are in bold letters. The ideal formula is $^{A}\mathbf{K}^{B}(\mathbf{NaCa})^{C}\mathbf{Mg}_5{}^{T}\mathbf{Si}_8\mathbf{O}_{22}{}^{W}(\mathbf{OH})_2$, which requires K_2O 5.65%, Na_2O 3.71%, CaO 6.72%, MgO 24.15%, SiO_2 57.60, H_2O 2.16, total 100.0 wt.%.

On back-scattered electron (BSE) images, with maximum contrast, a slight heterogeneity in the composition of the amphibole is indicated (Fig. 2). This is in part related to variations in the Mn and Na concentrations, also notable if the two sets of analyses in Table 1 are compared. To certify that the specimen is K-dominant throughout, EDS point analyses (20 kV, $n = 16$), were collected on different parts of six grains of potassic-richterite over an 8 × 10 mm area in the polished section of the type specimen. A wider concentration range of K_2O is observed, 3.0–3.8 wt%, but with an average value of 3.6 wt%, comparable to the WDS data (Table 1). PbO was not included in the original microprobe analysis, but occurs in variable amounts, corresponding to up to 0.02 atoms per formula unit (pfu). F is the most variable element, possibly related to analytical difficulties, but it is clearly established that OH > F in this sample. Li and B are only present in trace amounts.

Infrared spectroscopy and Mössbauer spectroscopy

A FTIR spectrum was collected on potassic-richterite powder (3 mg, mixed with KBr) in the range 600–4000 cm^{-1} at a spectral resolution of 2 cm^{-1} with a Bruker Vertex 70 spectrometer attached to a Bruker Hyperion 2000 IR-microscope. In the 600–1500 cm cm^{-1} range (Fig. 3) absorption bands are identified at 1145 cm^{-1}, 1077 cm^{-1}, 1043 cm^{-1}, 970 cm^{-1}, 957 cm^{-1}, 922 cm^{-1}, 740 cm^{-1}, 703 cm^{-1}, and 677 cm^{-1}. These values are very similar to infrared (IR) data presented for potassic-richterite from the Murun Massif (Chukanov 2014).

Polarised single-crystal FTIR spectra in the range 2000–8000 cm^{-1} were collected from a 56 μm thick doubly polished single-crystal fragment oriented parallel to (010), with the same instrument as mentioned above. The spectra (Fig. 4) show distinct absorption bands (with some shoulder features) at 3672 cm^{-1} and 3736 cm^{-1} in the α direction caused by O-H stretching vibrations of the OH dipole at the O(3) site. The two main bands represent the ^{A}□-MgMgMg-SiSi and ^{A}K-MgMgMg-SiSi arrangements, respectively, observed for nominal end-member synthetic potassic-richterite (Hawthorne et al. 1997; Hawthorne and Della Ventura 2007). Mottana and Griffin (1986) reported bands at similar wavenumbers for two samples of natural potassic-richterite, 3670 cm^{-1} and 3730 cm^{-1}. The band at 3736 cm^{-1} shows a minor shoulder at 3730 that is surely related to the ^{A}Na-MgMgMg-SiSi arrangement. Less evident is the extending asymmetry toward lower wavenumbers

Table 1 Results from EMPA analyses of potassic-richterite, with calculated cation proportions

Point*	0 $n = 3$	1	2	3	4	5	6	Average 1–6
EMPA results (wt%):								
SiO_2	55.99	56.42	55.78	56.27	56.44	55.98	55.31	56.03
Al_2O_3	0.39	0.20	0.24	0.21	0.21	0.23	0.29	0.23
TiO_2	0.00	0.00	0.04	0.00	0.02	0.02	0.00	0.01
Cr_2O_3	0.00	0.00	0.03	0.03	0.03	0.03	0.03	0.03
Fe_2O_3	1.65	2.10	2.03	1.98	1.72	1.97	2.11	1.99
MnO	5.22	4.88	4.79	4.21	3.95	4.51	4.51	4.48
NiO		0.00	0.01	0.01	0.00	0.03	0.08	0.02
MgO	20.92	20.09	20.08	20.51	20.61	20.50	20.39	20.36
CaO	5.52	5.04	5.06	5.17	5.52	5.15	5.10	5.17
SrO		0.04	0.11	0.01	0.05	0.00	0.00	0.04
BaO		0.05	0.03	0.00	0.00	0.05	0.00	0.02
Na_2O	4.98	5.41	5.45	5.44	4.93	5.26	4.93	5.24
K_2O	3.42	3.49	3.44	3.27	3.17	3.41	3.37	3.36
PbO		0.49	0.48	0.63	0.67	0.77	0.52	0.59
F	0.80	0.36	0.32	0.37	0.36	0.48	0.51	0.40
H_2O*	1.74	1.95	1.95	1.94	1.95	1.89	1.85	1.92
Total	100.63	100.53	99.89	100.06	99.64	100.28	99.05	99.91
O=F	0.34	0.15	0.14	0.16	0.15	0.20	0.21	0.17
Total including O=F	100.29	100.37	99.75	99.91	99.49	100.07	98.84	99.74
Calculated mineral formulae (apfu):*								
Si	7.902	7.98	7.94	7.97	8.00	7.94	7.91	7.96
Al	0.06	0.02	0.04	0.03	0.00	0.04	0.05	0.04
Total T-site cations	7.97	8.00	7.98	8.00	8.00	7.98	7.96	7.99
Ti^{4+}	0.00	0.00	0.00	0.00	0.00	0.00	0.00	0.00
Al^{VI}	0.00	0.01	0.00	0.01	0.04	0.00	0.00	0.00
Cr^{3+}	0.00	0.00	0.00	0.00	0.00	0.00	0.00	0.00
Fe^{3+}	0.18	0.22	0.22	0.21	0.18	0.21	0.23	0.21
Mn^{2+}	0.62	0.58	0.58	0.50	0.47	0.54	0.55	0.54
Mg	4.40	4.23	4.26	4.33	4.35	4.33	4.35	4.31
Ni^{2+}	0.00	0.00	0.01	0.01	0.00	0.02	0.05	0.01
Total C-site cations	5.20	5.05	5.08	5.06	5.06	5.11	5.19	5.08
Ca	0.83	0.76	0.77	0.78	0.84	0.78	0.78	0.79
Na	1.36	1.48	1.50	1.49	1.35	1.45	1.37	1.44
K	0.62	0.63	0.62	0.59	0.57	0.62	0.62	0.61
Pb		0.02	0.02	0.02	0.03	0.03	0.02	0.02
Ba	0.00	0.00	0.00	0.00	0.00	0.00	0.00	0.00
Sr	0.00	0.00	0.01	0.00	0.00	0.00	0.00	0.00
Total A, B-site cations	3.01	2.90	2.93	2.89	2.80	2.88	2.78	2.86
F	0.36	0.16	0.15	0.17	0.16	0.21	0.23	0.18
OH	1.64	1.84	1.85	1.83	1.85	1.79	1.77	1.82
Total W-site anions	2.00	2.00	2.00	2.00	2.00	2.00	2.00	2.00

*Point #0 is the average of three older EMP analyses. Points #1–6 represent analyses of the fragment used for single-crystal XRD study

**Calculated based on 24(O,OH,F) apfu (atoms per formula unit)

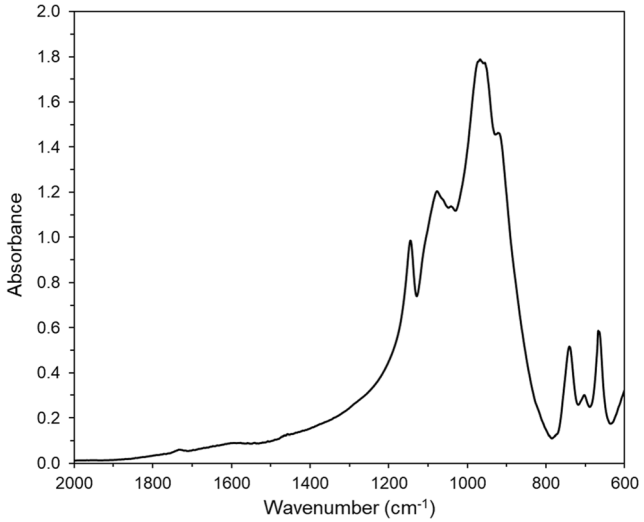

Fig. 3 Powder FTIR spectrum of potassic-richterite for the 600–2000 cm^{-1} range

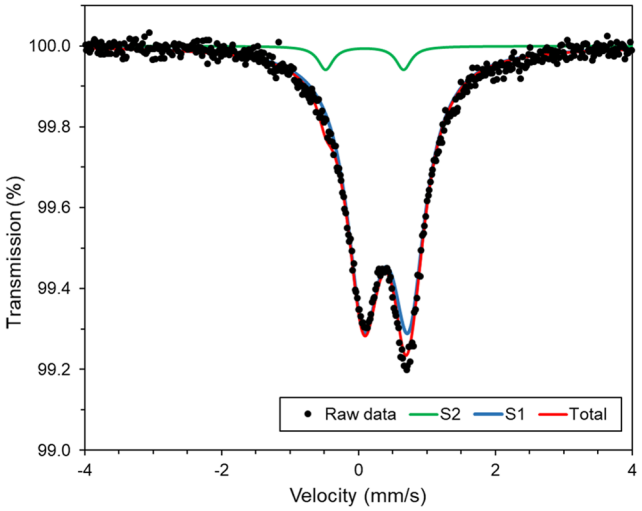

Fig. 5 Transmission ^{57}Fe Mössbauer spectrum of potassic-richterite. The fitted S1 and S2 subspectra correspond to $^{[6]}Fe^{3+}$ and $^{[4]}Fe^{3+}$, respectively

that should be related to the ^{A}K-MgMgMg-SiAl and ^{A}Na-MgMgMg-SiAl configurations (Hawthorne and Della Ventura 2007), in accordance with the crystal chemistry (< 2% $^{T(1)}$Al), see discussion below.

A sample of potassic-richterite was analyzed by Mössbauer spectroscopy using a conventional spectrometer system operated in constant-acceleration mode. Due to limited amounts of pure material, a ^{57}Co rhodium matrix point-source with a nominal activity of 0.37 GBq was used. The absorber was prepared by grinding a sample (ca 1 mg) together with a thermoplastic resin, which was then shaped to a ca 1-mm sized cylinder under mild heating (< 120 °C). The absorber was attached on strip tape and positioned close to the point source. The spectrum (Fig. 5) was collected for 900 h at room-temperature over 1024 channels, covering the velocity range −4.2 to +4.2 mm^{-1}, and was calibrated against an α-Fe foil. Spectrum analysis was done assuming Lorentzian line shapes

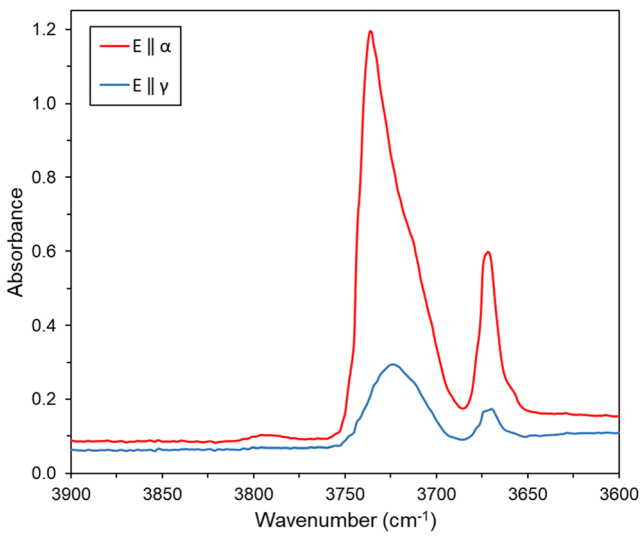

Fig. 4 Polarized single-crystal FTIR spectra of potassic-richterite in the O-H stretching region. E is the electric field vector

Table 2 X-ray powder diffraction pattern for potassic-richterite

d_{obs} (Å)	d_{calc} (Å)	I_{obs} (%)	I_{calc} (%)	h	k	l
9.05	9.02	5	44	0	2	0
8.55	**8.53**	**36**	**11**	**1**	**1**	**0**
4.51	4.51	8	37	0	4	0
4.27	4.27	4	3	2	2	0
3.40	3.40	20	100	1	3	1
3.303	**3.301**	**56**	**55**	**2**	**4**	**0**
3.181	**3.179**	**100**	**70**	**3**	**1**	**0**
2.970	2.971	15	31	2	2	1
2.847	**2.845**	**50**	**18**	**3**	**3**	**0**
2.756	2.756	18	32	-3	3	1
2.714	**2.714**	**37**	**98**	**1**	**5**	**1**
2.592	2.592	14	51	0	6	1
2.532	2.537	12	75	−2	0	2
2.407	2.406	12	7	3	5	0
2.353	2.352	23	40	−3	5	1
2.298	2.298	9	19	−1	7	1
2.173	2.174	25	34	2	6	1
2.035	2.036	7	7	3	5	1
1.927	1.926	22	8	5	1	0
1.667	1.668	27	28	4	6	1
1.650	1.650	10	6	4	8	0
1.617	1.617	12	5	1	11	0
1.521	1.520	5	7	1	9	2
1.513	1.512	6	24	−2	6	3
1.456	1.455	32	31	−6	6	1

The five strongest Bragg reflections are in bold

with the MossA program (Prescher et al. 2012). A relatively broad doublet (FWHM = 0.59) is dominant, with a centroid shift (CS) of 0.40(1) mm/s and quadrupole splitting (QS) of 0.65(1) mm/s, respectively, indicative of Fe^{3+} at octahedrally coordinated cation sites. A small contribution, ca 4% of total absorption, from another doublet at CS = 0.09(2) and QS = 1.14(6) mm/s is attributed to Fe^{3+} in tetrahedral coordination, in agreement with (Al + Si) ≤ 8 apfu in potassic-richterite. Any amount of Fe^{2+}, if present, is estimated to be less than 2% of all Fe. The final χ^2 value of the spectrum fit was 1.45.

X-ray diffraction data and structure refinement

X-ray powder diffraction data were recorded on a PANalytical X'Pert^3 Powder diffractometer equipped with an X'celerator silicon-strip detector and operated at 40 mA and 45 kV (Cu$K\alpha$-radiation, λ = 1.5406 Å). Peak positions were determined with the X'Pert HighScore Plus program and corrected against an external Si standard. Indexed *d* values and relative peak-heights above background are given in Table 2. The monoclinic unit-cell parameters, obtained by least-squares refinement of 22 reflections, are: a = 10.006(2) Å, b = 18.038(4) Å, c = 5.279(1) Å β = 104.5(3)° and V = 922.5(3) Å^3.

A single-crystal X-ray study was done on a 420 × 80 × 90 μm crystal using an Oxford Diffraction Xcalibur diffractometer, operating at 50 kV and 30 mA, with monochromatized MoK radiation and equipped with a CCD detector at 80 mm from the sample position. A combination of ω/φ scans, with a step scan of 1 ° and an exposure time of 25 s per frame at low theta angles and duplicating counting time at high theta angles, was used to maximize redundancy and data coverage. We collected high resolution data (up to 0.5 Å). Crystal data, including the refined unit-cell parameters, and experimental settings are summarized in Table 3.

The structure of potassic-richterite was refined starting from the atom coordinates of Oberti et al. (1992). Scattering curves for fully ionized chemical species were used at sites where chemical substitutions occur; neutral vs. ionized scattering curves were used at the T and anion sites [except O(3)]. Splitting of scattering at the sites M(4) and A was observed and added to the model as M(4′), A(*m*) and A(2) sites, respectively. A maximum close to O(3) (ca. 0.8 Å) was also observed in the Fourier difference map and added to the model as the hydrogen position. The positions of A(*m*) and A(2) sites were fixed during refinement and the hydrogen isotropic-displacement parameter was restrained to the displacement parameter of the anions at O(3). Full-matrix least-squares refinement on F^2 converged to R_{obs} = 3.64% (1811 reflections with $I_o > 2\sigma(I)$) and R_{all} = 6.23% (2399 reflections). Refined atom coordinates and equivalent isotropic-displacement parameters are reported in Table 4. The anisotropic-displacement parameters are given in Table S1 (electronic supplementary). Selected interatomic distances and angles are given in Table 5. Site populations for potassic-richterite were derived from the unit-formula and the results of the structure refinement, and are given in Table 6.

Table 3 Crystal data and structure refinement for potassic-richterite

Temperature (K)	293(2)
Wavelength (Å)	0.71073
Crystal system	Monoclinic
Space group	$C2/m$
a (Å)	9.9977(3)
b (Å)	18.0409(4)
c (Å)	5.2794(2)
β (°)	104.465(4)
V (Å^3)	922.05(5)
Z	2
Calculated density (g·cm^{-3})	3.075
Absorption coefficient (mm^{-1})	1.040
F(000)	868
Crystal size (mm^3)	0.42 × 0.09 × 0.08
Range of data collection (°θ)	3.99 to 45.62
Index ranges	$-18 \le h \le 18$, $-35 \le k \le 36$, $-7 \le l \le 6$
Reflections collected	19,458
Independent reflections	2399 [$R_{(int)}$ = 0.0391]
Completeness to theta = 25.00 ° (%)	99.4
Refinement method	Full-matrix least-squares on F^2
Data / restraints / parameters	2399 / 1 / 126
Goodness-of-fit on F^2	1.144
Final R indices [$I > 2\sigma(I)$]	$R1$ = 0.0363, w$R2$ = 0.0558
R indices (all data)	$R1$ = 0.0623, w$R2$ = 0.0631
Largest diffraction peak and hole (e·Å^{-3})	0.521 and − 0.525

On the basis of the observed mean bond lengths, and in agreement with what has been already observed by Oberti et al. (1993) for $^C Mn^{2+}$, the following (strong) Mn site preference is inferred: $M(2) >> M(1) > M(3)$. Fe^{3+} is also assumed to be ordered at the M(2) site, obtaining a site population of ($Mg_{1.41}Mn_{0.39}Fe^{3+}{}_{0.20}$). This leaves 0.08 Mn^{2+} to be assigned to M(1) and M(3) as well as 0.07 apfu at the M(4′) site (see below). According to Table 6, the composition of the M(1) site is ($Mg_{1.93}Mn^{2+}{}_{0.07}$) and M(3) is ($Mg_{0.97}Mn^{2+}{}_{0.03}$), leaving some Mn^{2+} to be allocated to M(4′).

The cations at the A sites are preferentially ordered. K plus some Na are ordered at A(*m*); the refined site-scattering at A(*m*) is 12.92 epfu, which corresponds to 0.61 K apfu and 0.14 Na apfu. The rest of Na is ordered at the A(2/*m*) site; the refined site-scattering at A(2/*m*) is 0.95 epfu, which accounts for 0.09 Na apfu. Regarding the A(2) subsite, the refined site scattering is 1.58 epfu, which accounts for 0.02 Pb apfu. Both K and Na contents at the A sites agree reasonably

Table 4 Refined atom coordinates and equivalent isotropic displacement parameters

Atom	Site occupancy	*x/a*	*y/b*	*z/c*	U_{eq}
O(1)	O^0 0.18(4) $O^=$ 0.82(4)	0.11078(9)	0.08613(4)	0.21789(19)	0.0077(2)
O(2)	O^0 0.14(4) $O^=$ 0.82(4)	0.11899(9)	0.17008(5)	0.72515(19)	0.0088(2)
O(3)	O^- 0.76(3) F^- 0.24(3)	0.10599(15)	0	0.7149(3)	0.0100(4)
O(4)	O^0 0.21(4) $O^=$ 0.79(4)	0.36222(10)	0.24756(5)	0.7947(2)	0.0124(2)
O(5)	O^0 0.27(4) $O^=$ 0.73(4)	0.34366(10)	0.12997(5)	0.0920(2)	0.0109(2)
O(6)	O^0 0.26(4) $O^=$ 0.74(4)	0.34035(10)	0.11635(5)	0.5911(2)	0.0109(2)
O(7)	O^0 0.26(6) $O^=$ 0.74(6)	0.33358(14)	0	0.2945(3)	0.0118(3)
T(1)	Si^0 0.62(3) Si^{4+} 0.38(3)	0.27584(4)	0.084927(16)	0.29666(8)	0.00652(9)
T(2)	Si^0 0.64(3) Si^{4+} 0.36(3)	0.28522(4)	0.171242(17)	0.80204(8)	0.00675(9)
M(1)	Mg^{2+} 0.960(3) Mn^{2+} 0.040(3)	0	0.08917(3)	½	0.0077(2)
M(2)	Mg^{2+} 0.692(3) Mn^{2+} 0.308(3)	0	0.18073(2)	0	0.00865(16)
M(3)	Mg^{2+} 0.973(4) Mn^{2+} 0.027(4)	0	0	0	0.0074(3)
M(4)	Ca^{2+} 0.51(3) Na^+ 0.42(7)	0	0.2774(3)	½	0.0135(5)
M(4′)	Mn^{2+} 0.06(2)	0	0.264(3)	½	0.015(3)
A(*m*)	K^+ 0.340(5)	0.0137	½	0.0347	0.0430(13)
A	Na^+ 0.087(14)	0	½	0	0.009
*A*2	Na^+ 0.072(7)	0	0.4669	0	0.043(8)
H	H 0.76(3)	0.181(6)	0.0000	0.755(10)	0.048(15)

well with the EPMA analysis, ($K_{0.61}Na_{0.30}Pb_{0.02}$). The chemical analyses indicate nearly full occupancy of the *A* sites (7% vacancy), and the above site assignment from structure refinement agrees well with this value. The nearly complete occupancy also indicated in the FTIR spectrum, where a weaker band is observed at 3672 cm^{-1}, compatible with a tremolite-like environment (i.e. $^{A}\square$-MgMgMg-SiSi). The existence of *A*(2) could be related to the presence of "small" divalent cations at the B position, but also to the ordering of Pb at the *A*-sites observed for joesmithite (Moore 1968, 1969) and plumboan pargasite (Hålenius and Bosi 2012), where the Pb atoms orders at the A sites and shifts away from the inversion center along the diad, in the case of joesmithite leading to a decrease in symmetry from *C*2/*m* to *P*2/*a* (Moore et al. 1993). There is a significant occupancy at the B-group by Mn^{2+}, which enters the *M*(4′) site displaced towards the strip of octahedra relative to the *M*(4) site, as observed by Oberti et al. (1993) in some samples of Mn-bearing richterite. The worst agreement between observed (refined) and calculated (assigned) site populations is observed for the *B* sites and *A* sites (Table 6), where differences of up to 7–8% are thought to be due to $NaMn^{2+}_{-1}$ variability between single analytical points (Table 1). Such a zonation is visible in Fig. 2.

The observed <*T*(1)-O> distance is somewhat longer than expected from the small amounts of Al^{3+} measured by EPMA analysis. The equation for calculating $^{T(1)}$Al from <*T*(1)-O> distance proposed by Oberti et al. (2007a) gives 0.13 apfu vs. the analysed amount of 0.04 apfu. Similar values of <*T*(1)-O> where reported for potassic-richterite by Oberti et al. (1992), although some of their crystals had slightly lower Al content (1.622 Å and 0.05 apfu Al in *T*(1)). Using the observed <*T*(2)-O> distance and the predictive equation of Oberti et al. (2007a), up to 0.19 apfu of Al in *T*(2) is indicated, which is not in agreement with the EPMA analysis. On the other hand, the EPMA analysis gave no Ti and a deficiency of Al + Si up to 0.04 apfu for certain points. If a large cation like Fe^{3+} is to occupy a T-site in richterite, following Oberti et al. (1992), it occurs at the *T*(2) site. This would certainly enlarge

Table 5 Selected interatomic distances and bond angles in potassic-richterite

Interatomic bond	Distance (Å)	Interatomic bond	Distance (Å)
T(1)–O(1)	1.598(1)	*T*(2)–O(2)	1.609(1)
T(1)–O(5)	1.629(1)	*T*(2)–O(4)	1.583(1)
T(1)–O(6)	1.629(1)	*T*(2)–O(5)	1.683(1)
T(1)–O(7)	1.638(1)	*T*(2)–O(6)	1.671(1)
<*T*(1)–O>	1.624	<*T*(2)–O>	1.636
M(1)–O(1) × 2	2.067 (1)	*M*(2)–O(1) × 2	2.197(1)
M(1)–O(2) × 2	2.062(1)	*M*(2)–O(2) × 2	2.102(1)
M(1)–O(3) × 2	2.097(1)	*M*(2)–O(4) × 2	2.000(1)
<*M*(1)–O>	2.075	<*M*(2)–O>	2.100
M(3)–O(1) × 4	2.080(1)	*M*(4)–O(2) × 2	2.419(4)
M(3)–O(3) × 2	2.046(1)	*M*(4)–O(4) × 2	2.364 (1)
<*M*(3)–O>	2.069	*M*(4)–O(5) × 2	2.866(2)
		M(4)–O(6) × 2	2.619(3)
A–O(5) × 4	2.951(1)	<*M*(4)–O>	2.567
A–O(6) × 4	3.145(1)		
A–O(7) × 2	2.545(1)	*M*(4′)–O(2) × 2	2.19 (5)
<*A*–O>	2.937	*M*(4′)–O(4) × 2	2.327(4)
		M(4′)–O(5) × 2	3.04(4)
A(2)–O(5) × 2	2.472(1)	*M*(4′)–O(6) × 2	2.84(5)
A(2)–O(6) × 2	2.783(1)	<$^{[6]}$*M*(4′)–O>	2.567
A(2)–O(7) × 2	2.614(2)	<$^{[8]}$*M*(4′)–O>	2.600
<*A*(2)–O>	2.623		
		Interatomic bond	Angle (°)
A(*m*)–O(5) × 2	2.956(1)	*T*(1)–O(5)–*T*(2)	136.20(7)
A(*m*)–O(5) × 2	2.908(1)	*T*(1)–O(6)–*T*(2)	136.01(7)
A(*m*)–O(6) × 2	3.000(1)	*T*(1)–O(7)–*T*(1)	138.5(1)
A(*m*)–O(7)	2.521(2)	O(5)–O(6)–O(5)	169.27(6)
A(*m*)–O(6) × 2	3.297(1)	O(6)–O(7)–O(6)	107.10(8)
A(*m*)–O(7)	2.584(2)		
<*A*(*m*)–O>	2.943		
O(3)–H	0.73(6)		

the size of the *T*(2) tetrahedron, even for a very low amount, justifying the observed <*T*(2)-O > distance (1.636 Å), that is slightly larger than observed for the ^{IV}Ti-free richterite samples studied by Oberti et al. (1992). Although the amount is so low that it is within the error of the analytical methods, the fitting of a weak $^{IV}Fe^{3+}$ doublet to the Mössbauer spectrum seems to agree well with this hypothesis.

Petrogenesis

Potassic-richterite is a rare member of the amphibole supergroup but occurs over a wide range of geological environments and *P*-*T* conditions. Common features are silica undersaturation and peralkaline bulk compositions of the rock system, although a few exceptions to this are found. The high-*T* and high-*P* stability, relevant for upper mantle conditions, has been studied in some detail (e.g. Konzett et al. 1997; Trønnes 2002). Overall, the thermal stability increases as a function of increasing *P*, and K-rich compositions tend to persist to higher *P* and *T*. There is also experimental evidence that an increase of the F/OH ratio stabilizes potassic-(fluoro-)richterite to higher *T* (Foley 1991). More generally, successful synthesis of near end-member potassic-richterite has been done from 700 °C and at standard conditions of *P* = 1–2 kbar (H_2O), with good yields and few microstructural defects (e.g, Zimmermann et al. 1997; Hawthorne et al. 1997). However, a small excess of Ca (i.e, a tremolite component) is not uncommon in synthetic samples (e.g., Melzer et al. 2000). Data on the stability and phase relations at lower *T* and *P* are apparently missing. The assemblage with potassic-richterite from a blueschist facies terrain (Mottana and Griffin 1986) suggests that formation is possible at lower *T*, < 450 °C.

It is probable that different sources of key elements contributed to the eventual formation of potassic-

Table 6 Site populations for potassic-richterite

Site	Site population (apfu)	ss (epfu)		mbl (Å)	
		refined	calculated	refined	calculated
T(1)	3.96 Si^{4+} + 0.04 Al^{3+}			1.624	1.623
T(2)	3.98 Si^{4+}+ 0.02 Fe^{3+}			1.636	
M(1)	1.93 Mg^{2+} + 0.07 Mn^{2+}	25.04	24.91	2.075	2.073
M(2)	1.41 Mg^{2+} + 0.39 Mn^{2+}+ 0.20 Fe^{3+}	32.00	31.87	2.100	2.098
M(3)	0.97 Mg^{2+} + 0.03 Mn^{2+}	12.35	12.39	2.069	2.075
Σ C cations		69.40	69.17		
B cations	1.14 Na + 0.07 Mn^{2+} + 0.79 Ca^{2+}	32.64	30.09		
A cations	0.61 K^{+} + 0.30 Na^{+}+ 0.02 Pb^{2+}	15.45	16.53		
W anions	1.82 OH + 0.18 F	16.48	16.18		

There is a good agreement between the refined values of site-scattering (ss) - given in electrons per formula unit (epfu) - and mean bond-lengths (mbl, in Å), and those calculated based on the proposed site populations

richterite. The marble-ore precursors contain the necessary Ca, Mg and Si, with additional Mn, Fe and Pb, in the Långban-type deposits (Magnusson 1930; Holtstam and Mansfeld 2001). K, Na and to some extent Si, have likely been added from fluids via metasomatic alteration of the felsic volcanic beds. At Pajsberg, potassic-richterite most probably crystallized during the main skarn-forming process, synchronous with Svecokarelian ~1.85 Ga peak regional metamorphism, inferred at temperatures of ca 700 °C and pressures of 3–6 kb in this part of Bergslagen (Stephens et al. 2009). These conditions are similar to the estimates of Grew et al. (1994), $P \leq 4$ kbar, $T \geq 500$ °C, and of Christy and Gatedal (2005), $P = 3$ kbar, $T > 600$ °C, for skarns in the Långban deposit, 13 km N of Pajsberg. It is possible that the mineralization also was affected by contact metamorphism from a small body of metabasite in the immediate vicinity of the Pajsberg field, appearing along the contact between the metavolcanic country rock and the metacarbonate host (Björck 1986). As estimated from the association of potassic-richterite with tephroite and Mn^{3+}-bearing jacobsite, oxygen fugacity during mineral formation was above the magnetite stability field but well below that of bixbyite (Brusnitsyn 2007). As noted, the type specimen is free of Ti, in contrast to most samples of potassic-richterite from mantle-derived rocks. Due to geometrical constrains, Ti incorporation at the $T(2)$ site is believed to be favoured by dominance of K at the A site (Oberti et al. 2007b).

Metamorphic amphiboles with $^{[A]}K > {}^{[A]}Na$ are generally rare, and in a collection of more than 250 analyses of sodium-calcium amphiboles from metamorphic assemblages, only a handful were observed to contain >0.3 K atoms pfu (Schumacher 2007). The K/Na ratios of richterite essentially depends on the activity ratio of these elements in the mineral-forming fluid system (Zimmermann et al. 1997; Safonov and Butvina 2016). For K-rich amphibole compositions to form, it is probably critical that SiO_2 and Al_2O_3 are low, so that K is not bound up in other silicate minerals such as K-feldspar or trioctahedral mica.

The paragenetic relations and premetamorphic precursors to potassic-richterite in the present occurrence cannot be determined with certainty. It is possible that the mineral formed from direct reactions between phlogopite, dolomite and quartz, also involving a Na-rich fluid; however, the very low Al content of the amphibole produced remains to be explained. Another scenario is that an alkali-rich hydrothermal fluid has reacted with pre-existing tephroite and dolomite during the skarn-forming process, giving potassic-richterite and jacobsite.

Acknowledgements We thank the proton beamline facility (LIBAF) staff at Lund University for assisting with light-element analyses. The paper benefited from reviews by Frank C. Hawthorne and an anonymous expert, and comments from journal editor Nikita V. Chukanov.

References

Björck L (1986) Beskrivning till berggrundskartan Filipstad NV. Sveriges geologiska undersökning. Series Af. Berggrundsgeologiska och geofysiska kartor 147:110

Boström K, Rydell H, Joensuu O (1979) Långban - an exhalative sedimentary deposit? Econ Geol 74:1002–1011

Brusnitsyn AI (2007) Associations of Mn-bearing minerals as indicators of oxygen fugacity during the metamorphism of metalliferous deposits. Geochem Int 45:345–363

Christy AG, Gatedal K (2005) Extremely Pb-rich rock-forming silicates including a beryllian scapolite and associated minerals in a skarn from Långban, Värmland, Sweden. Mineral Mag 69:995–1018

Chukanov NV (2014) Infrared spectra of mineral species: extended library. Springer, Dordrecht

Dawson JB, Smith JV (1982) Upper-mantle amphiboles: a review. Mineral Mag 45:35–46

De La Rosa N, Kristiansson P, Nilsson EJC, Ros L, Elfman M, Pallon J (2017) Lithium analysis using a double-sided silicon strip detector at LIBAF. Nucl Instrum Meth B 404:29–33

Della Ventura G, Parodi GC, Maras S, Mottana A (1992) Potassium-fluor-richterite, a new amphibole from San Vito, Monte Somma, Campania, Italy. Rend Lincei-Sci Fis 3:239–245

Erlank AJ, Finger LW (1970) The occurrence of potassic-richterite in a mica nodule from the Wesselton kimberlite, South Africa. Carnegie I Wash 68:320–324

Foley S (1991) High-pressure stability of the fluor- and hydroxy-endmembers of pargasite and K-richterite. Geochim Cosmochim Acta 55:2689–2694

Grew ES, Yates MG, Belakovskiy DI, Rouse RC, Su SC, Marquez N (1994) Hyalotekite from reedmergnerite-bearing peralkaline pegmatite, Dara-i-Pioz, Tajikistan and from Mn skarn, Långban, Värmland, Sweden: a new look at an old mineral. Mineral Mag 58:285–297

Hålenius U, Bosi F (2012) Cation ordering in Pb^{2+}-bearing, Mn^{3+}-rich pargasite from Långban, Sweden. Am Mineral 97:1635–1640

Hamberg A (1890) Über krystallisirtes Blei von der Grube Harstigen bei Pajsberg in Wermland nebst Bemerkungen über die Paragenesis der begleitenden Mineralien. Zeitschrift für Krystallographie und Mineralogie 17:253–263

Hawthorne FC, Della Ventura G (2007) Short range order in amphiboles. In: Hawthorne FC, Oberti R, Della Ventura G, Mottana A (eds) Amphiboles: crystal chemistry, occurrence and health issues. Rew Mineral Geochem, vol 67. Mineral Soc Am, Chantilly, pp 173–222

Hawthorne FC, Della Ventura G, Robert J-L, Welch MD, Raudsepp M, Jenkins DM (1997) A Rietveld and infrared study of synthetic amphiboles along the potassium-richterite-tremolite join. Am Mineral 82:708–716

Hawthorne FC, Oberti R, Harlow GE, Maresch WV, Martin RF, Schumacher JC, Welch MD (2012) Nomenclature of the amphibole supergroup. Am Mineral 97:2031–2048

Hogarth DD (1997) Mineralogy of leucite-bearing dykes from Napoleon Bay. Baffin Island; multistage Proterozoic lamproites. Can Mineral 35:53–78

Holtstam D, Mansfeld J (2001) Origin of a carbonate-hosted Fe-Mn-(Ba-As-Pb-Sb-W) deposit of Långban-type in Central Sweden. Mineral Deposita 36:641–657

Igelström LJ (1867) Sällsynta och nya mineralier från Vermland: manganepidot, richterit eller manganhornblende, kataspilit och hyalophan. Öfversigt af Kongl. Vetenskaps-Akademiens Förhandlingar 24:11–18

Konzett J, Sweeney RJ, Thompson AB, Ulmer P (1997) Potassium amphibole stability in the upper mantle: an experimental study in a peralkaline KNCMASH system to 8. 5 GPa. J Petrol 38:537–568

Magnusson NH (1930) Långbans malmtrakt. Sveriges geologiska undersökning. Series Ca. Avhandlingar och uppsatser 23:111

Mandarino J (1981) The Gladstone-Dale relationship: part IV. The compatibility concept and its application. Can Mineral 19:441–450

Mazdab FK (2003) The diversity and occurrence of potassium-dominant amphiboles. Can Mineral 41:1329–1344

Melzer S, Gottschalk M, Andrut M, Heinrich W (2000) Crystal chemistry of K-richterite-richterite-tremolite solid solutions: a SEM, EMP, XRD, HRTEM and IR study. Eur J Mineral 12:273–291

Mitchell RH (2012) Kimberlites, orangeites, and related rocks. Springer, New York

Moore PB (1968) Joesmithite, a new amphibole-like mineral from Långban. Ark Mineral Och Geol 4:487–492

Moore PB (1969) Joesmithite: a novel amphibole crystal chemistry. Mineral Soc Am Spec Pap 2:111–115

Moore PB, Davis AM, Van Derveer DG, Sen Gupta PK (1993) Joesmithite, a plumbous amphibole revisited and comments on bond valences. Miner Petrol 48:97–113

Mottana A, Griffin WL (1986) Crystal chemistry of two coexisting K-richterites from St. Marcel (Val d'Aosta, Italy). Am Mineral 71: 1426–1433

Nilsson EJC, Kristiansson P, Ros L, De La Rosa N, Elfman M, Hålenius U, Pallon J, Skogby H (2017) A nuclear geochemical analysis system for boron quantification using a focused ion beam. J Radioanal Nucl Chem 311:355–364

Oberti R, Ungaretti L, Canillo E, Hawthorne FC (1992) The behaviour of Ti in amphiboles: I. Four- and six-coordinate Ti in richterite. Eur J Mineral 4:425–439

Oberti R, Hawthorne FC, Ungaretti L, Canillo E (1993) The behaviour of Mn in amphiboles: Mn in richterite. Eur J Mineral 5:43–51

Oberti R, Hawthorne FC, Cannillo E, Cámara F (2007a) Long-range order in amphiboles. In: Hawthorne FC, Oberti R, Della Ventura G, Mottana A (eds) Amphiboles: crystal chemistry, occurrence and health issues. Rew Mineral Geochem, vol 67. Mineral Soc Am, Chantilly, pp 125–172

Oberti R, Della Ventura G, Cámara F (2007b) New amphibole compositions: natural and synthetic. In: Hawthorne FC, Oberti R, Della Ventura G, Mottana A (eds) Amphiboles: crystal chemistry, occurrence and health issues. Rew Mineral Geochem, vol 67. Mineral Soc Am, Chantilly, pp 89–124

Prescher C, McCammon C, Dubrovinsky L (2012) MossA: a program for analyzing energy-domain Mössbauer spectra from conventional and synchrotron sources. J Appl Crystallogr 45:329–331

Safonov OG, Butvina VG (2016) Indicator reactions of K and Na activities in the upper mantle: natural mineral assemblages, experimental data. and thermodynamic modeling Geochem Int 54:858–872

Schumacher JC (2007) Metamorphic amphiboles: composition and coexistence. In: Hawthorne FC, Oberti R, Della Ventura G, Mottana A (eds) Amphiboles: crystal chemistry, occurrence and health issues. Rew Mineral Geochem, vol 67. Mineral Soc Am, Chantilly, pp 359–416

Sokolova EV, Kabalov Yu K, McCammon C, Schneider J, Konev AA (2000) Cation partitioning in an unusual strontian potassic-richterite from Siberia: Rietveld structure refinement and Mössbauer spectroscopy. Mineral Mag 64:19–23

Stephens MB, Ripa M, Lundström I, Persson L, Bergman T, Ahl M, Wahlgren CH, Persson PO, Wickström L (2009) Synthesis of the bedrock geology in the Bergslagen region, Fennoscandian Shield, south-central Sweden. Sveriges geologiska undersökning. Series Ba, Översiktskartor med beskrivningar 58:259

Sundius N (1945) The position of richterite in the amphibole group. Geol Foren Stock For 67:266–270

Trønnes RG (2002) Stability range and decomposition of potassic-richterite and phlogopite end members at 5–15 GPa. Miner Petrol 74:129–148

Wagner C, Velde D (1986) The mineralogy of K-richterite-bearing lamproites. Am Mineral 71:17–37

Yang H, Konzett J, Prewitt CT, Fei Y (1999) Single-crystal structure refinement of synthetic ^{M4}K-substituted potassic-richterite, $K(KCa)Mg_5Si_8O_{22}(OH)_2$. Am Mineral 84:681–684

Zimmermann R, Gottschalk M, Heinrich W, Franz G (1997) Experimental Na-K distribution between amphiboles and aqueous chloride solutions, and mixing model along the richterite – K-richterite join. Contrib Mineral Petrol 126:252–264